CHAPTER IV

RESULTS AND DISCUSSIONS

4.1 Use the MODFLOW program to prove the scaling law

From Chapter III, the MODFLOW program has been used to simulate the centrifuge model test patterns. In this section, centrifuge model tests have been simulated to support the scaling law by considering their velocity and hydraulic dispersion in the different types of media.

4.1.1 Silica Flour test

Four of the Silica Flour tests are simulated in this study. The prototype represented by these four models is shown in Figure 4.1. The model simulation is defined in Figure 4.2; a one dimension is simulated.

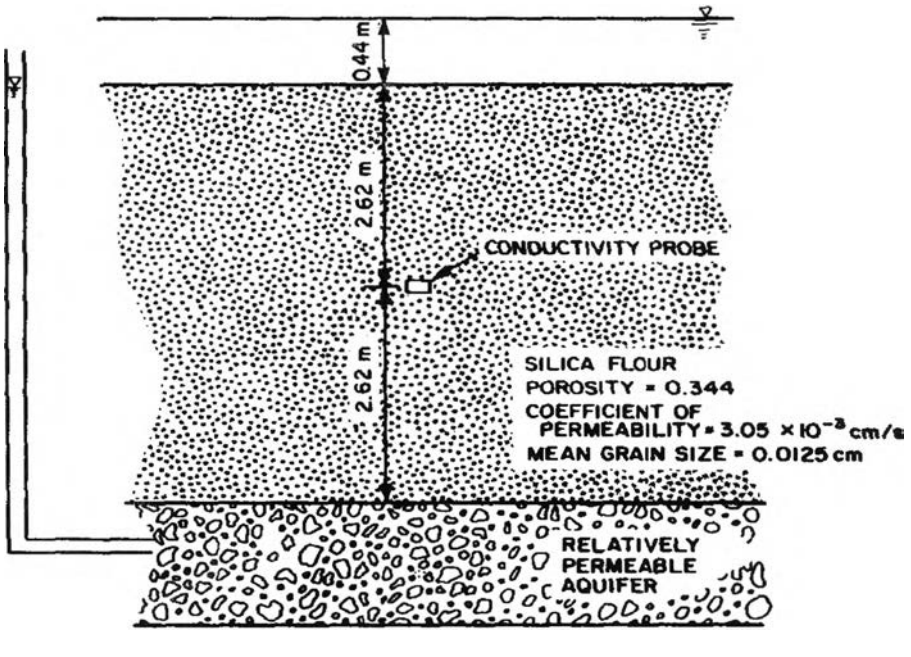

Figure 4.1 The prototype represented by four Silica Flour models
(From Arulanandan et al., 1988)

The boundary condition of each test is set as follows;

Constant Head

Left side: start and stop time head = 0.50m

Right side: start and stop time head = 0.06m

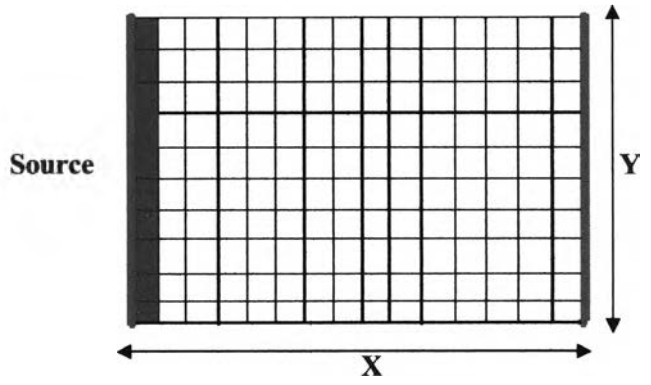

Figure 4.2 Solution domain for contaminant movement in Silica Flour test

At time t equal to 0 sec, the model is full with Silica Flour. Then the contaminant release from the point source and the observation concentration well is added at the middle of the pathway of each model to monitor the concentration of the contaminant.

After input all the parameters into the MODFLOW program, the next step is to run the model. The method that uses in this study is Hybrid MOC/MMOC. The result of the concentration before calibrating the dispersion is shown in Figure 4.3.

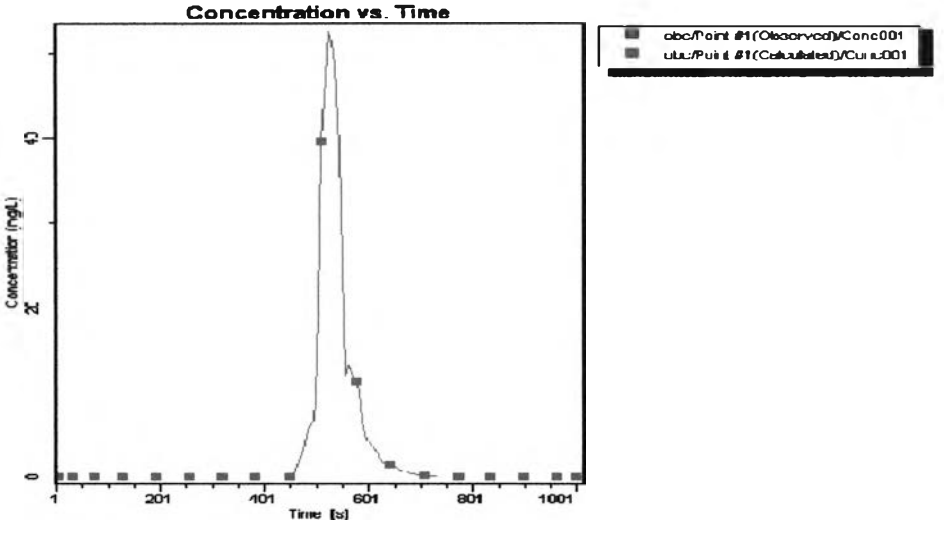

Figure 4.3 The concentration of Silica Flour versus time at 25g with no dispersion

After calibrate the K (Conductivity constant) and dispersion, the result of Silica Flour model at 25g is shown in Figure 4.4, as the concentration of the contaminant from the point source release to the observation concentration well.

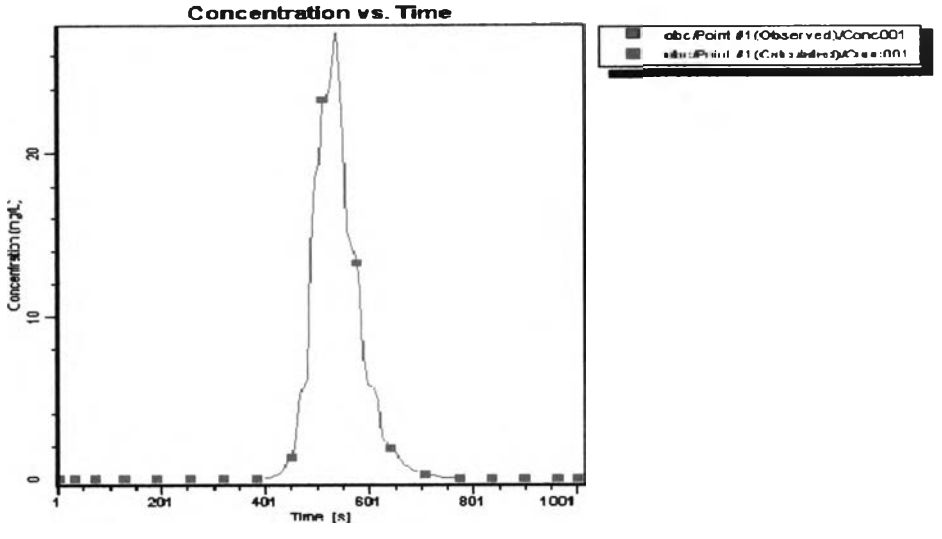

Figure 4.4 The concentration of Silica Flour versus time at 25g with calibrates the dispersion

From the result above, the data is used to make the breakthrough curve of the Silica Flour model at 25 g. The result is shown in Figure 4.5.

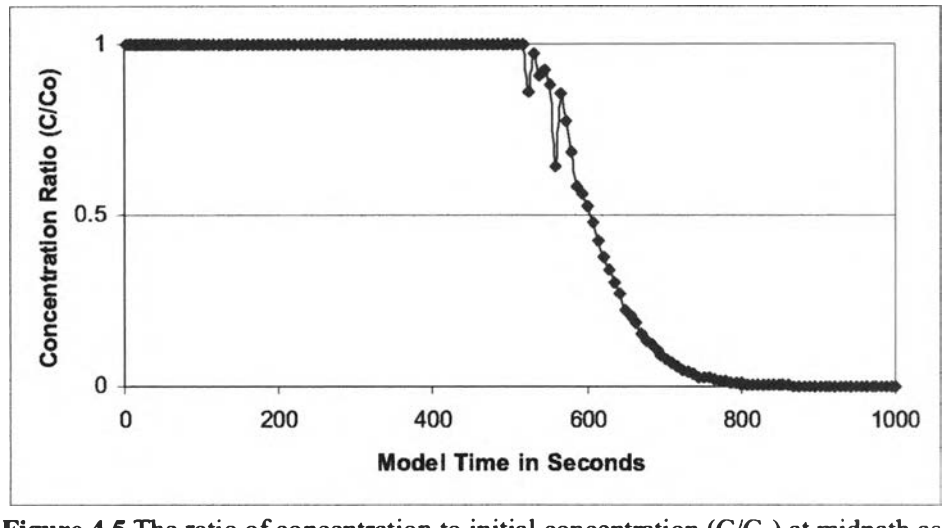

Figure 4.5 The ratio of concentration to initial concentration (C/C_0) at midpath as function of model time for Silica Flour model at 25g

Finally, the breakthrough curves for all the Silica Flour tests are predicted as shown in Figure 4.6, 4.7, 4.8 and 4.9. Please note that the test at 100g was not actually carried out, but only simulated in MODFLOW to check the validity of scaling laws.

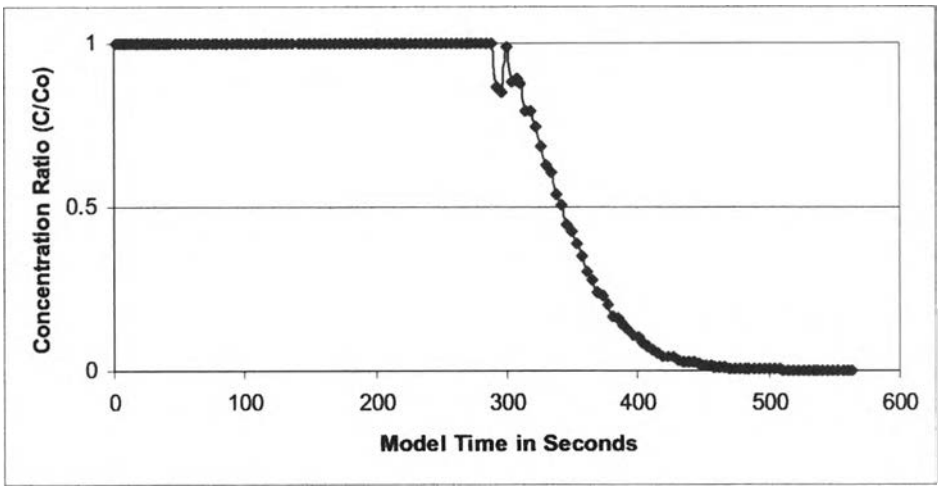

Figure 4.6 The ratio of concentration to initial concentration (C/C_0) at midpath as function of model time for Silica Flour model at 33.3g

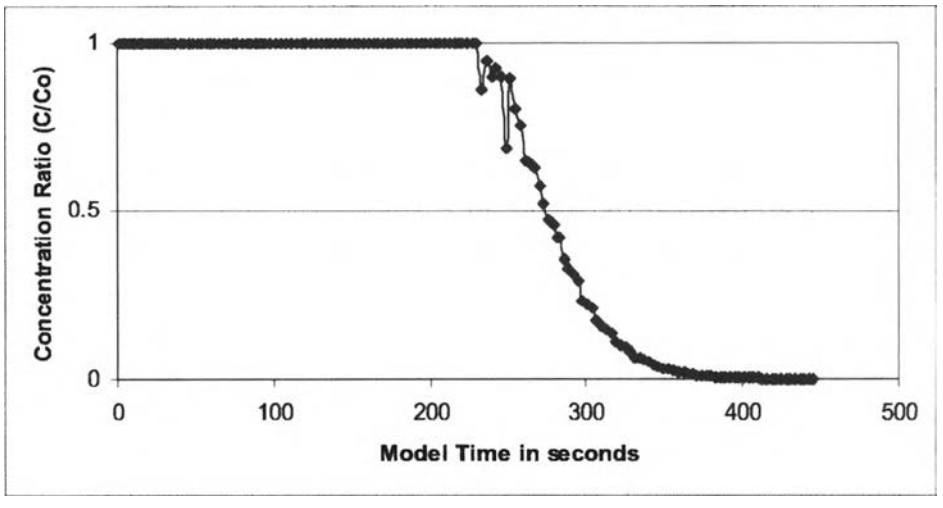

Figure 4.7 The ratio of concentration to initial concentration (C/C_0) at midpath as function of model time for Silica Flour model at 37.5g

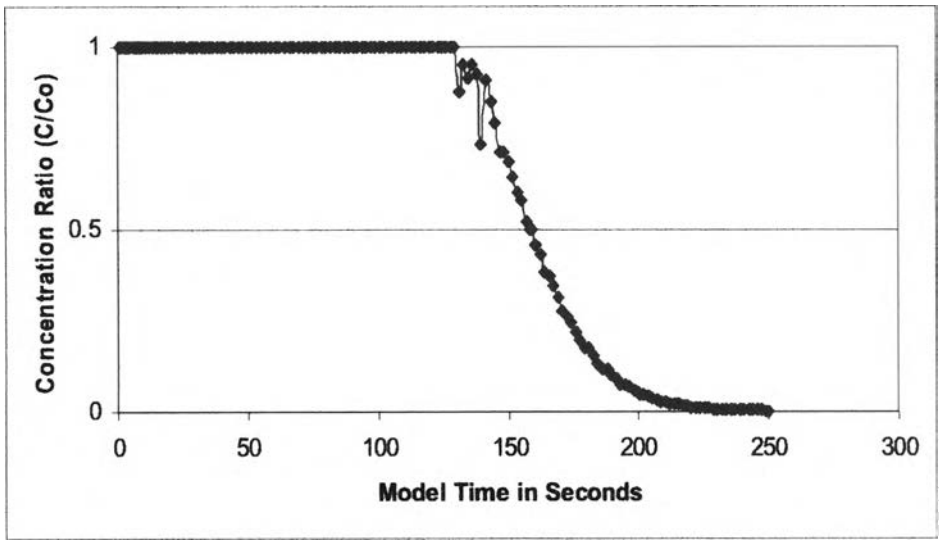

Figure 4.8 The ratio of concentration to initial concentration (C/C_0) at midpath as function of model time for Silica Flour model at 50g

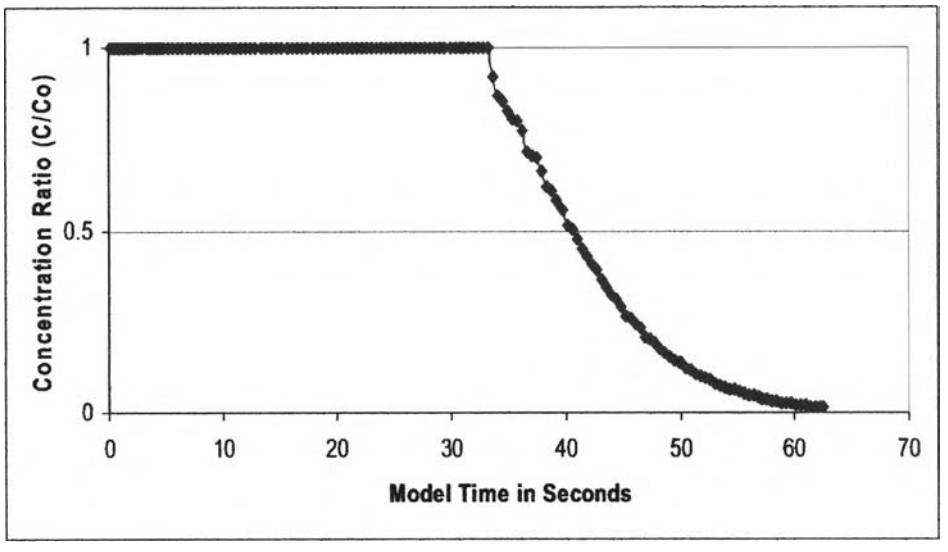

Figure 4.9 The ratio of concentration to initial concentration (C/C_0) at midpath as function of model time for Silica Flour model at 100g

After Silica Flour test, the data is ploted into the scale. The ratio of concentration to initial concentration (C/C_0) at middepth for all these four models is shown in Figure 4.10.

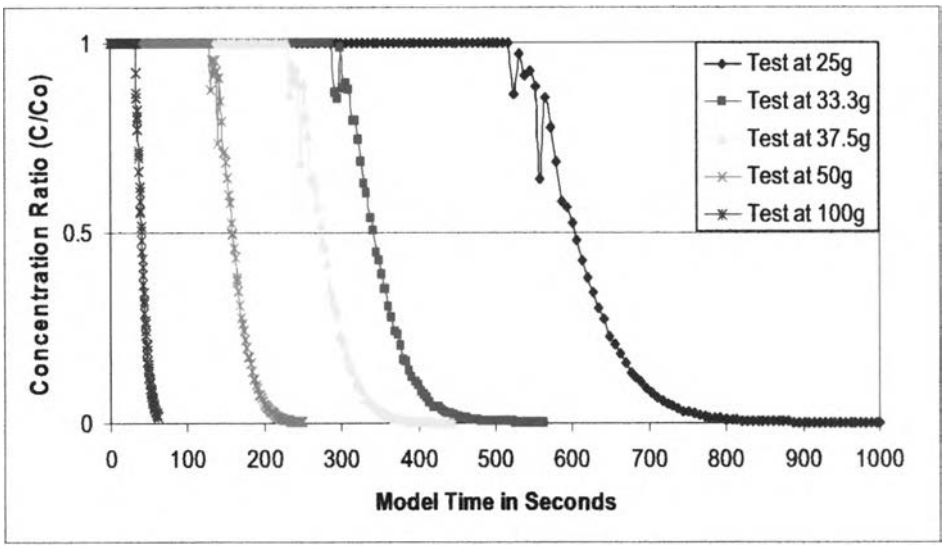

Figure 4.10 The ratio of concentration to initial concentration (C/C_0) at midpath as function of model time for Silica Flour models

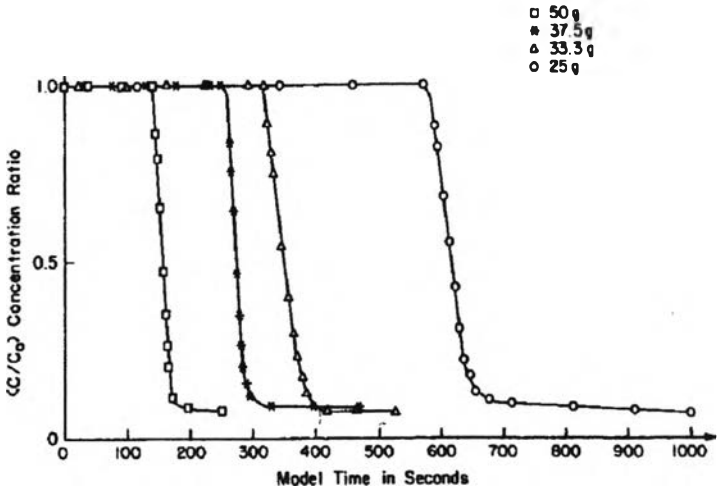

Figure 4.11 The ratio of concentration to initial concentration (C/C_0) at midpath as function of model time for Silica Flour models (From Arulanandan et al., 1988)

A plot of log t_m versus log N is shown in Figure 4.12, where t_m is the time taken for 50% reduction in concentration at midpath and N is the model scale factor.

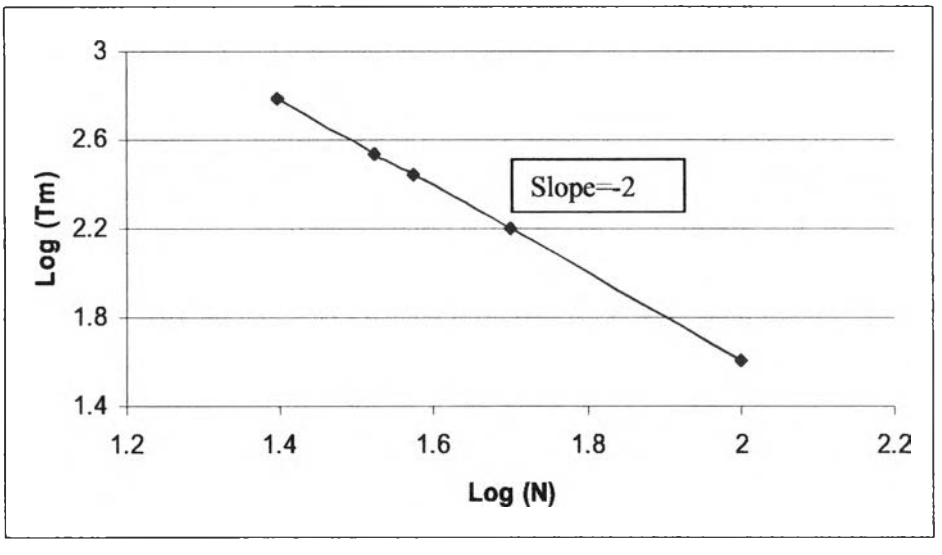

Figure 4.12 The logarithm of time for 50% reduction in concentration ratio at midpath versus logarithm of scale factor for Silica Flour model

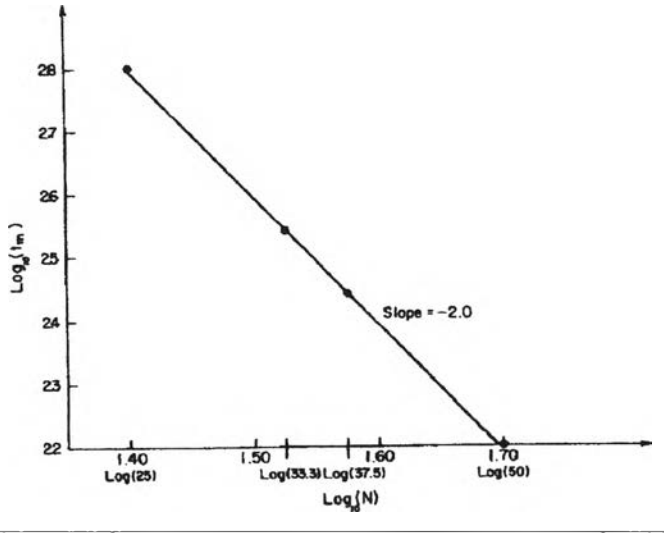

Figure 4.13 The logarithm of time for 50% reduction in concentration ratio at midpath versus logarithm of scale factor for Silica Flour model (From Arulanandan et al., 1988)

From Figure 4.12, the slope of the graph equal to -2 that will verify the $t^* = 1/N^2$ scaling law derived earlier in Chapter II.

The relationship between C/C_0 at midpath and the prototype time for these four models is shown in Figure 4.14. Prototype time is obtained using the relationship $t_p = N^2 t_m$, where subscripts p and m stand for prototype and model, respectively.

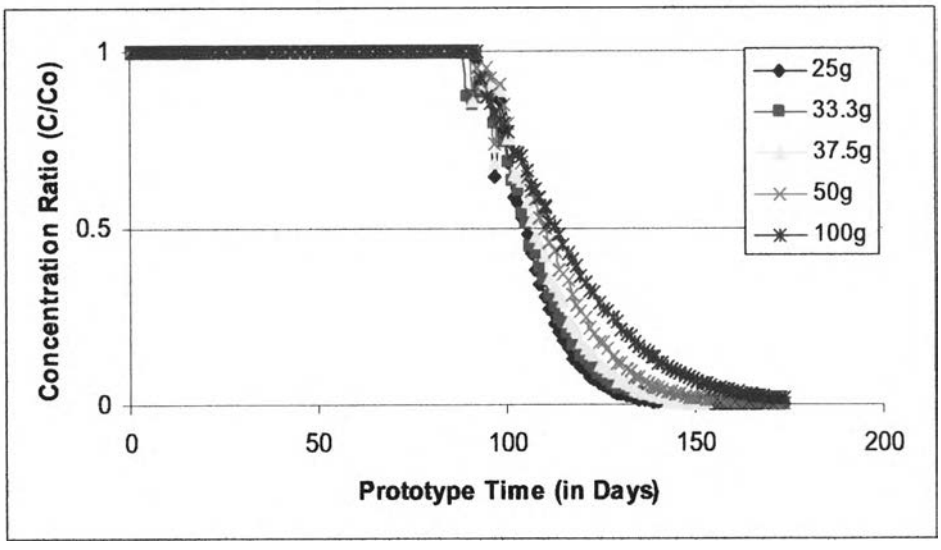

Figure 4.14 The ratio of concentration to initial concentration (C/C_0) at midpath as function of prototype for Silica Flour models

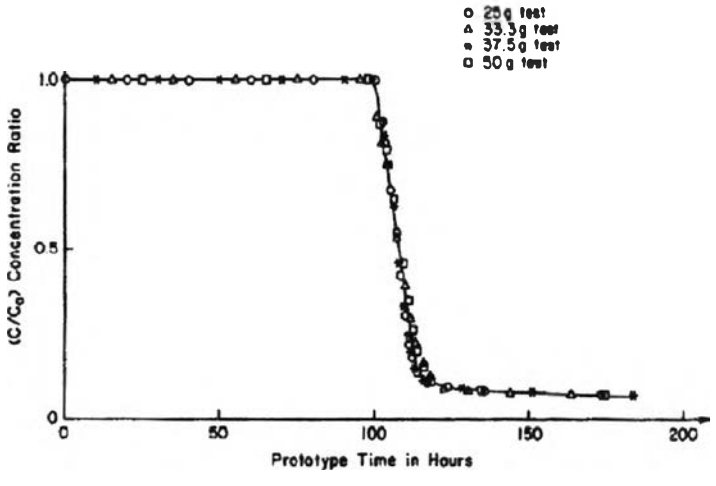

Figure 4.15 The ratio of concentration to initial concentration (C/C_0) at midpath as function of prototype for Silica Flour models (From Arulanandan et al., 1988)

Since all four models gave essentially the same behavior, it could be concluded that the scaling laws derived appear to be valid.

4.1.2 Clays test

Two centrifuge tests are carried out on 100% Snowcal 50 models with the centrifugal accelerations of 50g and 100g, respectively. The model simulation is defined in Figure 4.16; a one dimension is simulated.

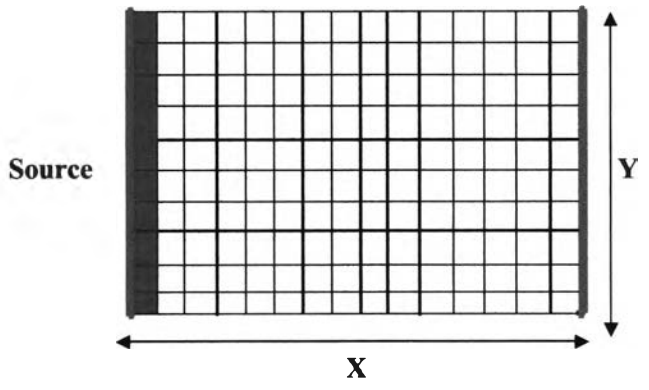

Figure 4.16 Solution domain for contaminant movement in Clays test

The boundary condition of each test is set as follows;

Constant Head

Left side: start and stop time head = 11m

Right side: start and stop time head = 0.84m

At time t equal to 0 sec, the model is full with 100% Snowcal 50. Then the contaminant release from the point source and the observation concentration well is added at the middle of the pathway of each model to monitor the concentration of the contaminant.

After input all the parameters into the MODFLOW program, the next step is to run the model. The method that uses in this study is Hybrid MOC/MMOC. The result of the concentration before calibrates the adsorption is shown in Figure 4.17.

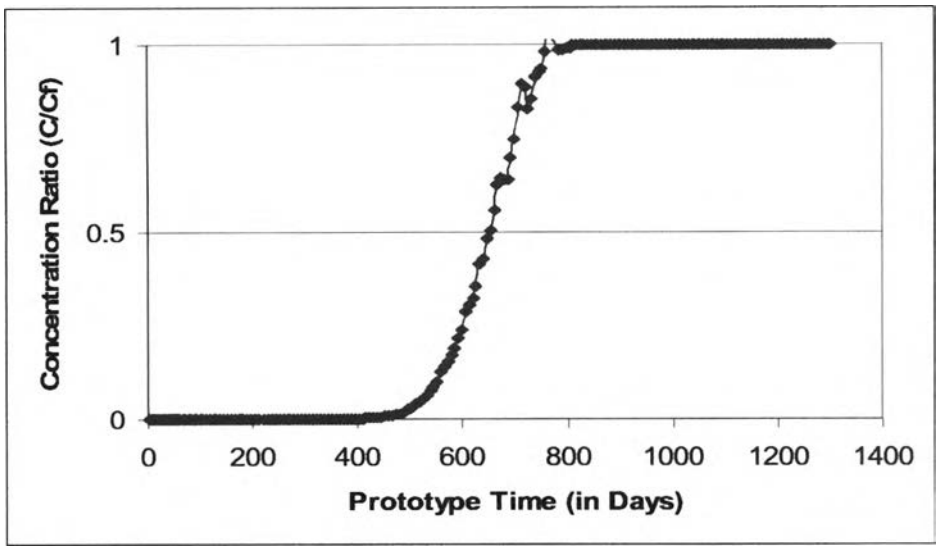

Figure 4.17 The ratio of concentration to final concentration (C/C_f) at midpath as function of prototype for Snowcal 50 model at 100g with no adsorption

Then, adsorption value is calibrated and the distribution coefficient (Kd) [1/(mg/L)] or SP1 = $6x10^{-8}$. The result of K_d is used to verify model to achieve another result. The breakthrough curve of 100% Snowcal 50 at 100g and 50g are shown in Figure 4.18 and 4.19.

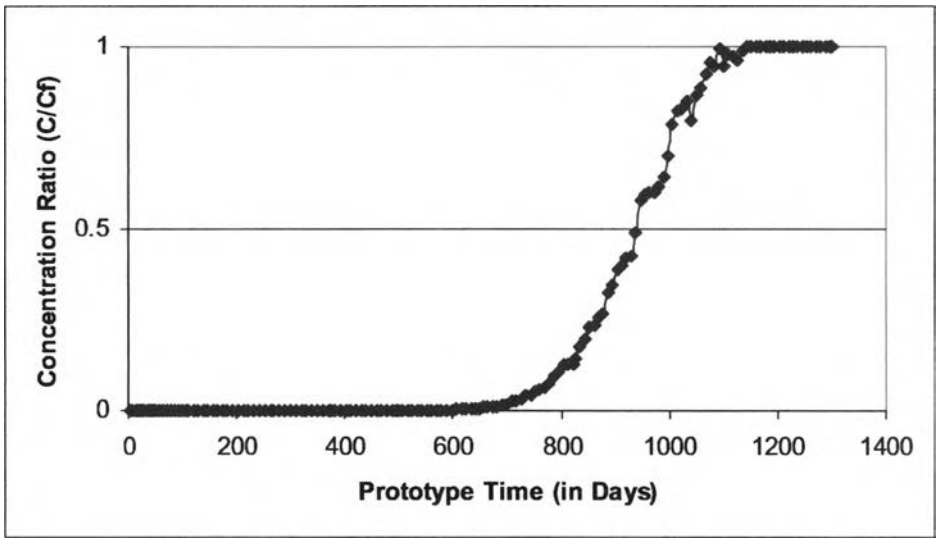

Figure 4.18 The ratio of concentration to final concentration (C/C_f) at midpath as function of prototype for Snowcal 50 model at 100g

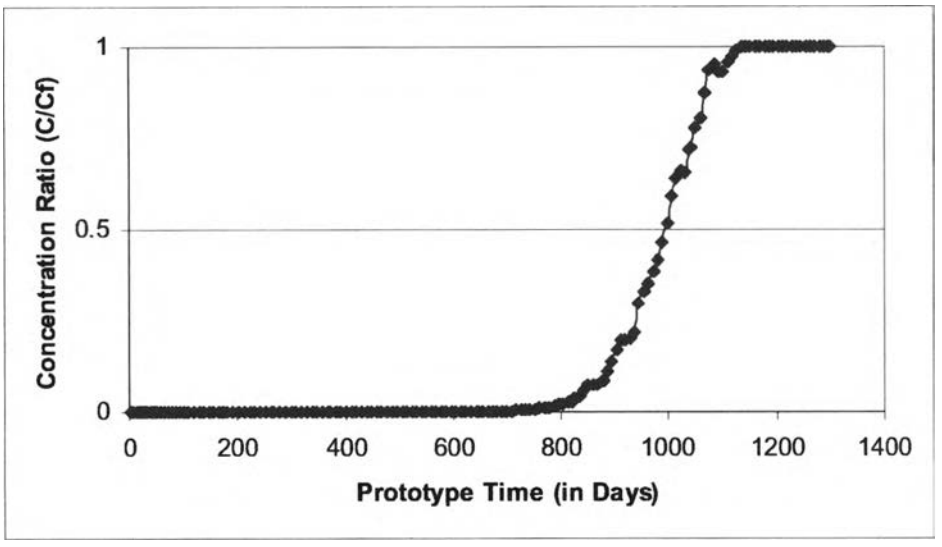

Figure 4.19 The ratio of concentration to final concentration (C/C_f) at midpath as function of prototype for Snowcal 50 model at 50g

After achieve all the result of the 100% Snowcal 50 model, plot all the data into the scale. The ratio of concentration to final concentration (C/C_f) at midpath is measured for all these three models is shown in Figure 4.20.

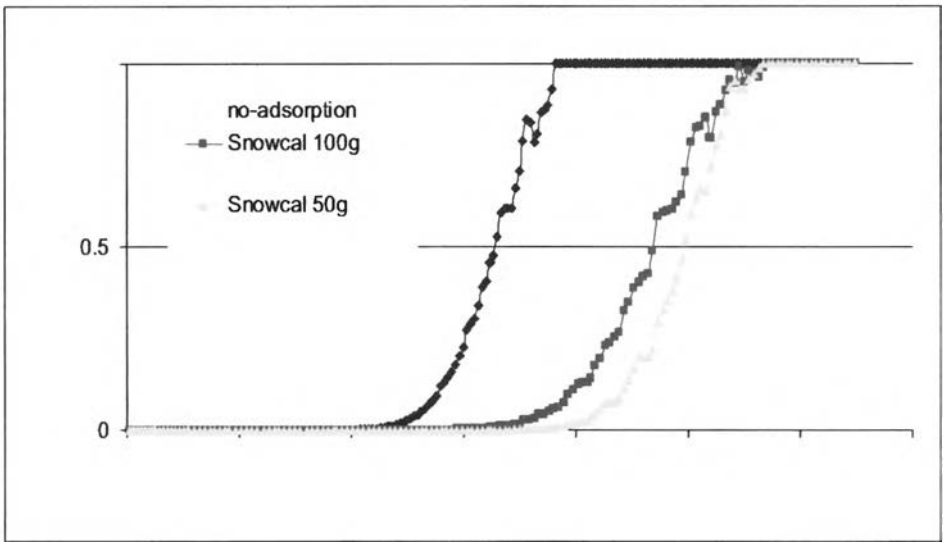

Figure 4.20 The ratio of concentration to final concentration (C/C_f) at midpath as function of prototype for Snowcal 50 models

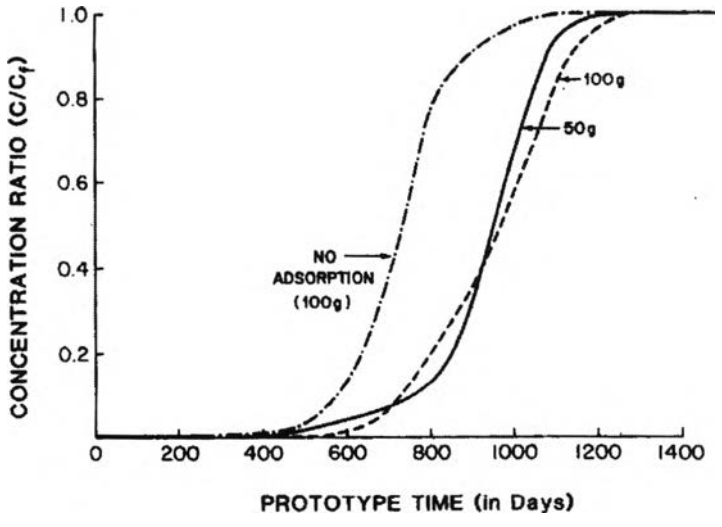

Figure 4.21 The ratio of concentration to final concentration (C/C_f) at midpath as function of prototype for Snowcal 50 models (From Arulanandan et al., 1988)

From Figure 4.20, the curve with no-adsorption is the curve deduced from the measured variation of C/C_f with time during leaching with alcohol. From Figure 4.17, adsorption retards the movement of the solute. Curves of 50g and 100g model, which represent the same prototype behavior, seem to agree reasonably well. The maximum variation between these curves is about 70 days prototypes time. This corresponds to 0.672 hour for the 50g model. This is slightly compared to the 12 hour (1250 days prototype time) duration of the test. Thus, it can be concluded that the scaling laws derived are supported.

4.1.3 Monterey 0/30 sand test

In this model, to study the influence of velocity on the hydraulic dispersion and two sets of the tests are performed on Monterey 0/30 sand.

Part 1: In this study, a sample of height of 0.208m with the observation concentration well at the mid-path is tested at 25g acceleration with varying excess pressure heads. The model simulation is defined in Figure 4.22; a one dimension is simulated.

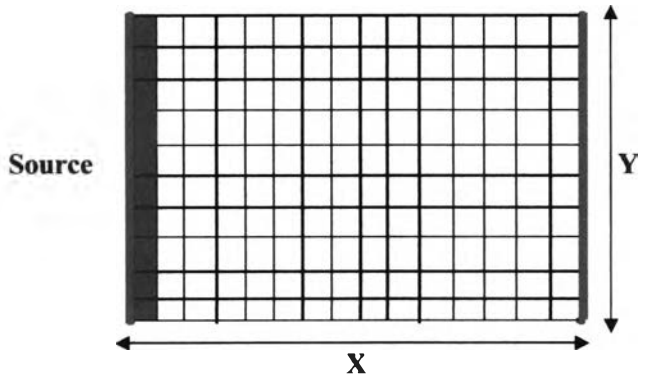

Figure 4.22 Solution domain for contaminant movement in Monterey 0/30 sand test

The boundary condition of each test is set as follows;

Constant Head

Left side: start and stop time head = (Varying with $\bar{v}$ of each test)

Right side: start and stop time head = (Varying with $\bar{v}$ of each test)

At time t equal to 0 sec, the model is full with Monterey 0/30. Then the contaminant release from the point source and the observation concentration well is added at the middle of the pathway of each model to monitor the concentration of the contaminant.

After input all the parameters into the MODFLOW program, the next step is to run the model. The method that uses in this study is Hybrid MOC/MMOC. The result of the concentration ratio is shown in Figure 4.23, 4.24 and 4.25.

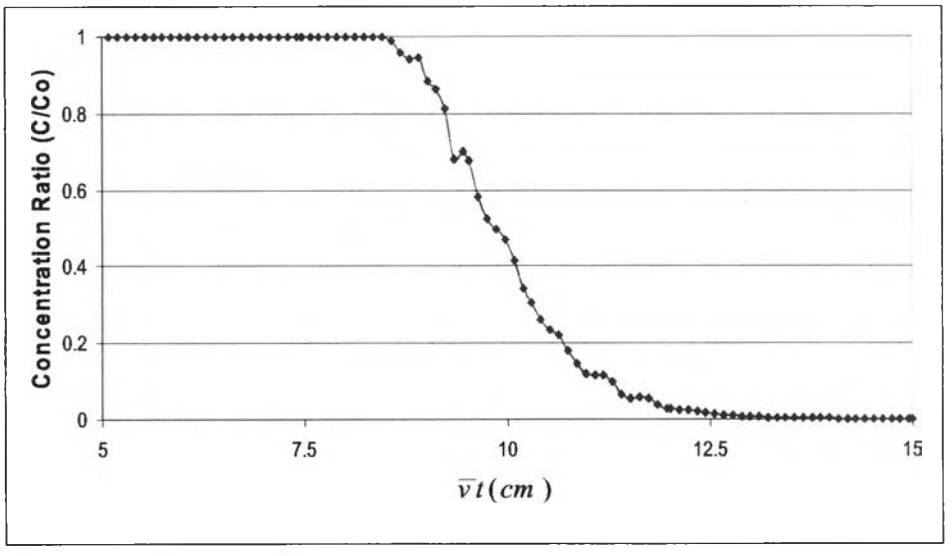

Figure 4.23 The ratio of concentration to initial concentration (C/C_0) at midpath as function of $\bar{v}t$ (where $\bar{v}$ = average interstitial velocity and t = model time) for Monterey 0/30 sand model test at 25g with $\bar{v}$ = 0.137 cm/sec

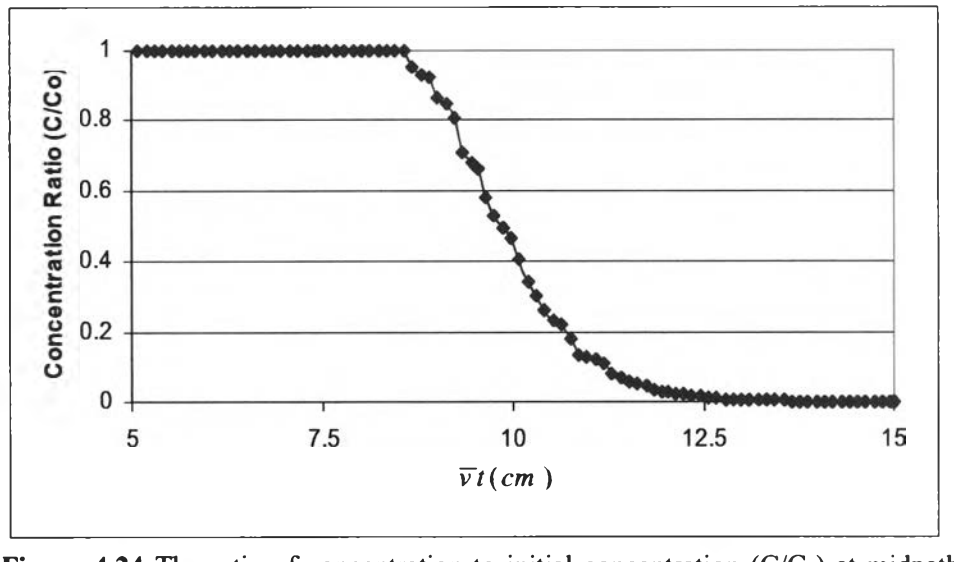

Figure 4.24 The ratio of concentration to initial concentration (C/C_0) at midpath as function of $\bar{v}t$ for Monterey 0/30 sand model test at 25g with $\bar{v}$ = 0.117 cm/sec

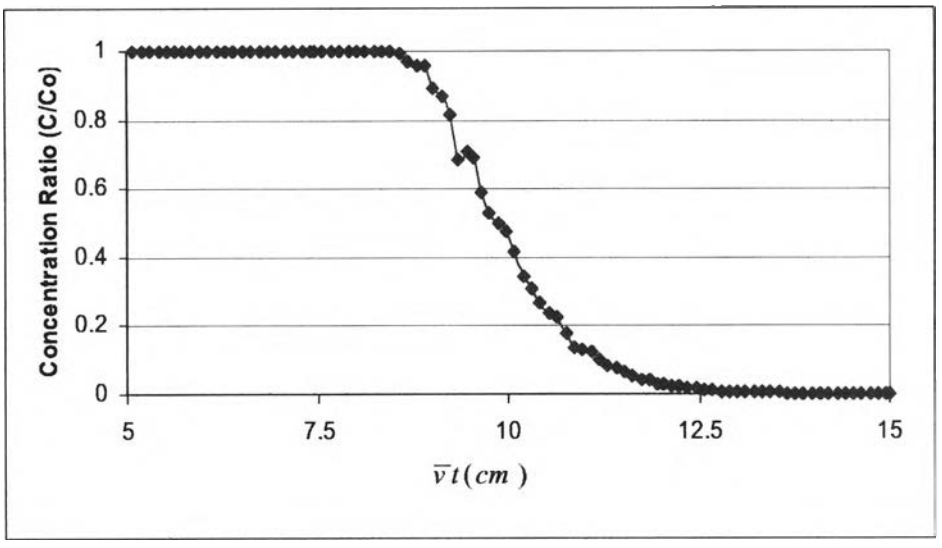

Figure 4.25 The ratio of concentration to initial concentration (C/C_0) at midpath as function of $\bar{v}t$ for Monterey 0/30 sand model test at 25g with $\bar{v}$ = 0.104 cm/sec

After achieve all the result of the Monterey 0/30sand test, plot all the data into the scale. The ratio of concentration to initial concentration (C/C_0) at midpath is measured for all these three models is shown in Figure 4.26.

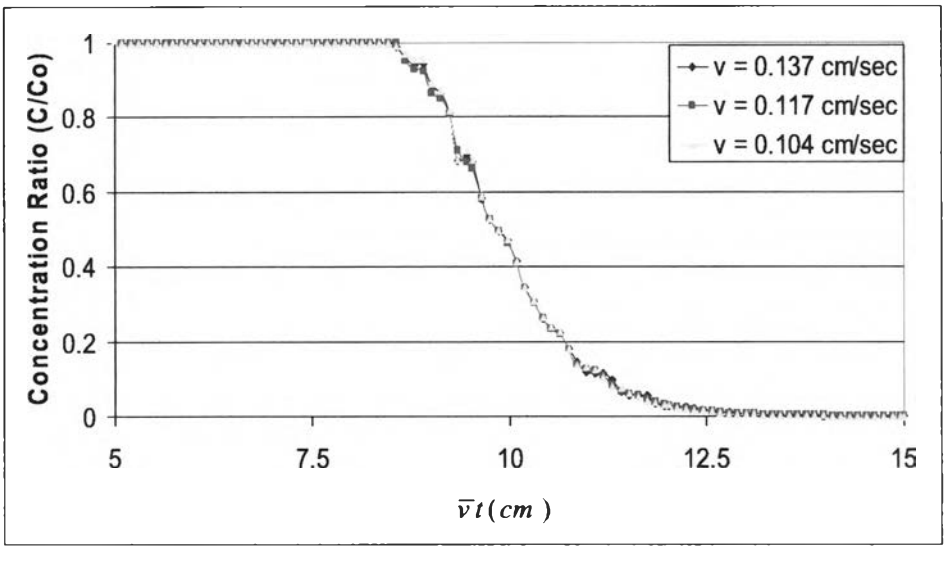

Figure 4.26 The ratio of concentration to initial concentration (C/C_0) at midpath as function of $\bar{v}t$ for Monterey 0/30 sand model test at 25g with varying average interstitial velocities

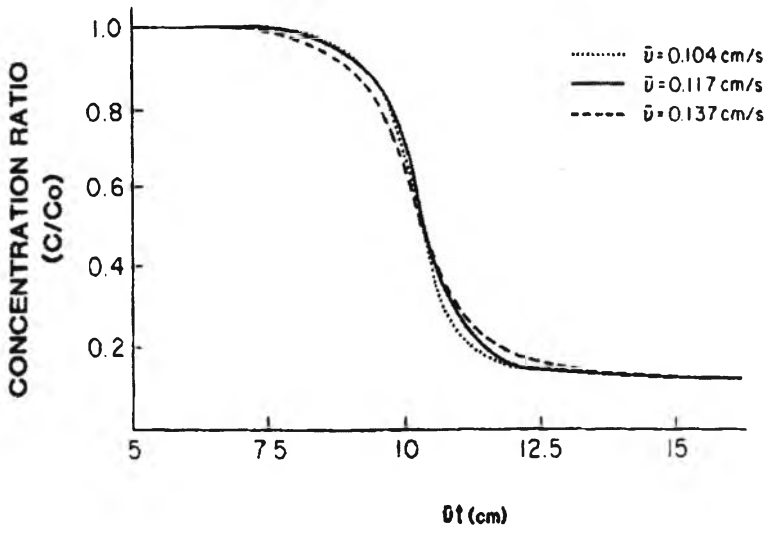

Figure 4.27 The ratio of concentration to initial concentration (C/C_0) at midpath as function of $\bar{v}t$ for Monterey 0/30 sand model test at 25g with varying average interstitial velocities (From Arulanandan et al., 1988)

From the figure 4.26 show that the velocity increase with increasing of the spreading of the breakthrough curves, including an increase in the hydrodynamic dispersion with an increase in the velocity. However, the differences are not significant due to the small range of average velocities used in these tests.

Part 2: This set of tests is performed in 1g acceleration. In this study, three samples with the observation concentration well at the midpath are subjected to different average interstitial velocities. The relationships between C/C_0 and $\bar{v}t/l$ for these tests are shown in Figure 4.28, 4.29 and 4.30, where l is the distance to the observation concentration well.

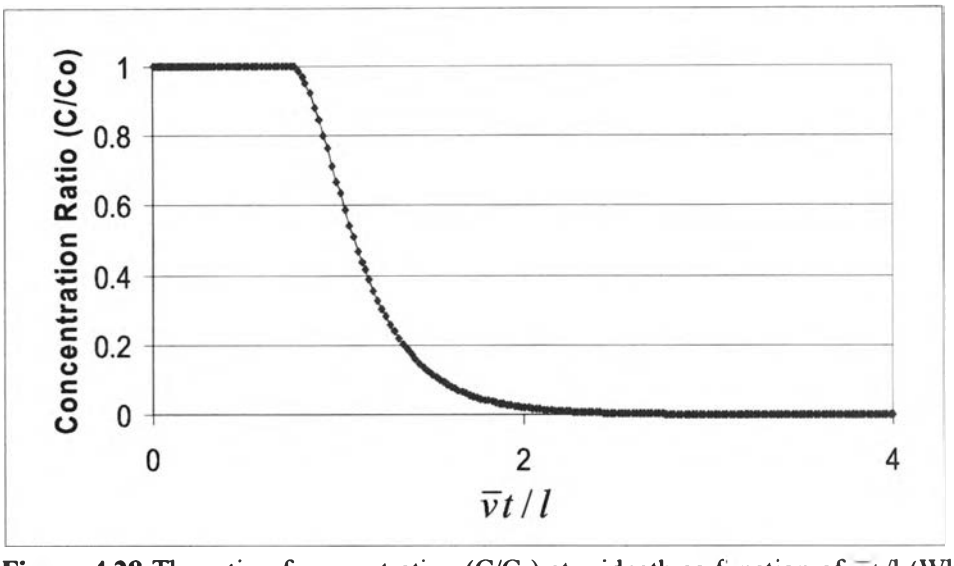

Figure 4.28 The ratio of concentration (C/C_0) at midpath as function of $\bar{v}t/l$ (Where $\bar{v}$ = average interstitial velocity; t = model time; and l = middepth) for Monterey 0/30 sand models test at 1g with sample thickness and $\bar{v}$ = 0.036 cm/sec

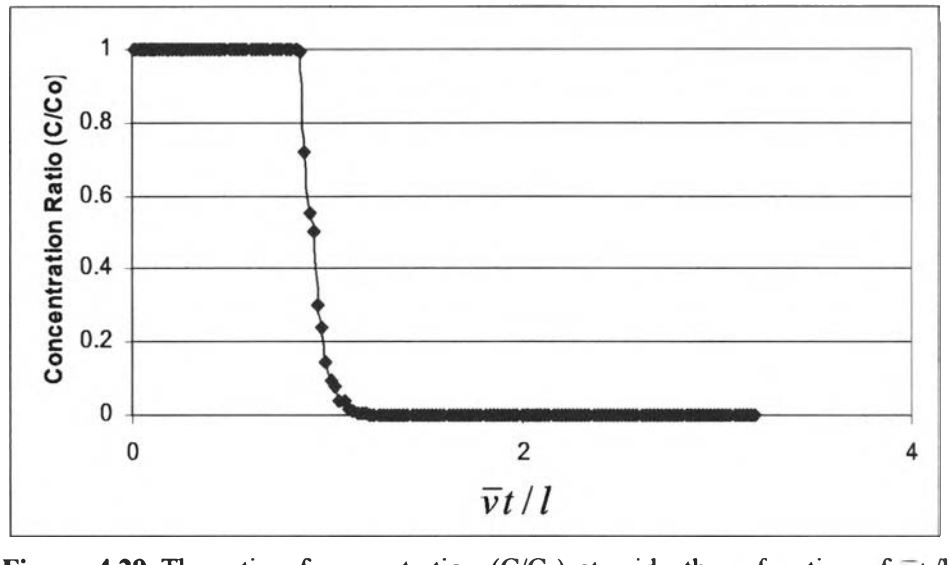

Figure 4.29 The ratio of concentration (C/C_0) at midpath as function of $\bar{v}t/l$ for Monterey 0/30 sand models test at 1g with sample thickness and $\bar{v}$ = 0.02 cm/sec

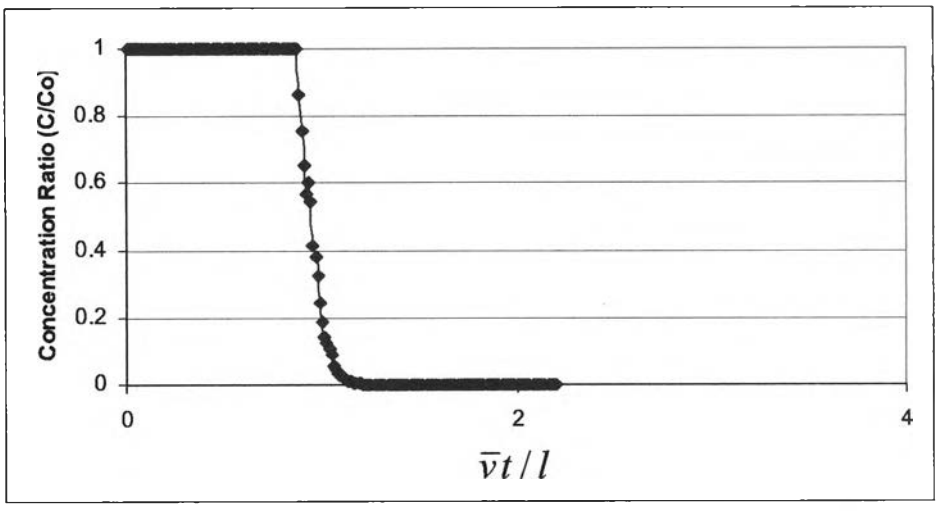

Figure 4.30 The ratio of concentration (C/C_0) at midpath as function of $\bar{v}t/l$ for Monterey 0/30 sand models test at 1g with sample thickness and $\bar{v}$ = 0.013 cm/sec

After achieve all the result of the Monterey 0/30sand test, plot all the data into the scale. The ratio of concentration to initial concentration (C/C_0) at midpath is measured for all these three models is shown in Figure 4.31.

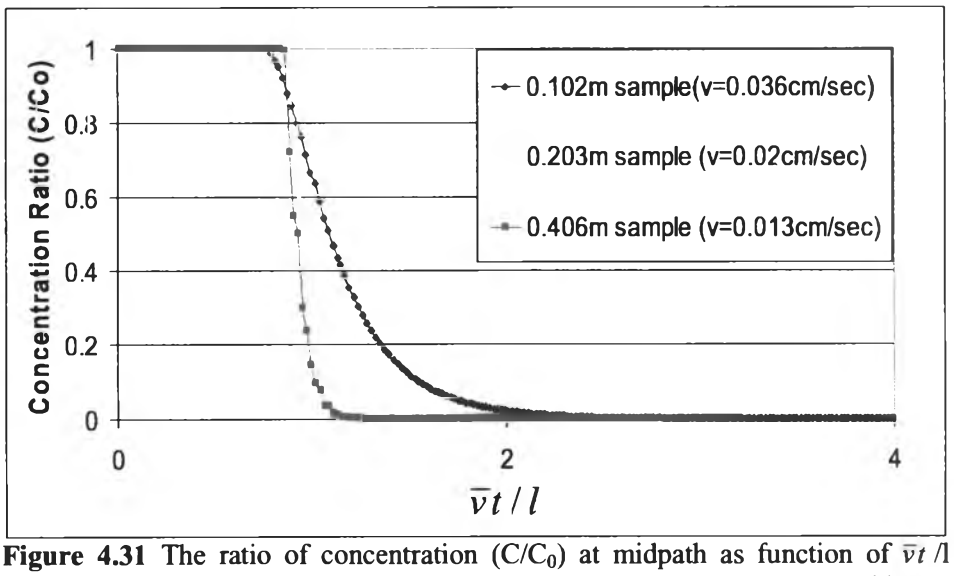

Figure 4.31 The ratio of concentration (C/C_0) at midpath as function of $\bar{v}t/l$ for Monterey 0/30 sand models testat 1g with varying sample thickness and with varying average interstitial velocities

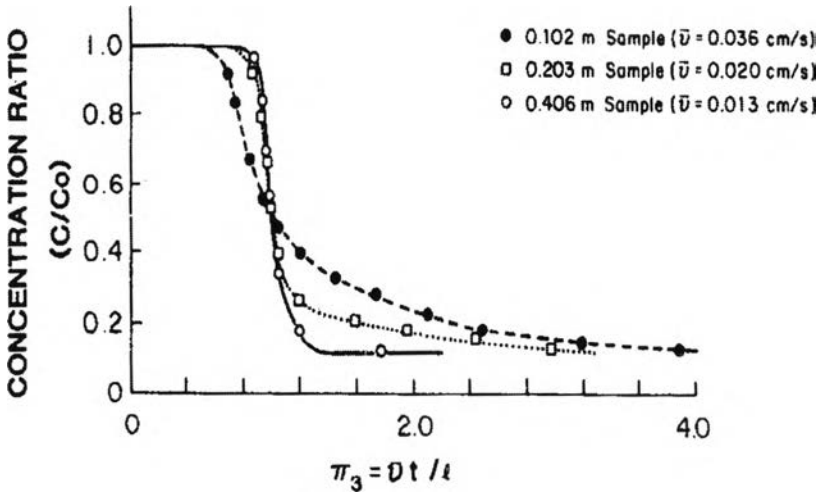

Figure 4.32 The ratio of concentration (C/C_0) at midpath as function of $\bar{v}t/l$ for Monterey 0/30 sand models test at 1g with varying sample thickness and with varying average interstitial velocities (From Arulanandan et al., 1988)

From the Figure 4.26, as the velocity increase, hydrodynamic dispersion also increases. The spreading of dispersion curves with increase in velocity is more prominent in 1g test than the centrifuge test due to the bigger range of velocities used.

4.2 Compare with experimental results

The prototype considered is a 10m wide landfill leaking dense pollutant through its base into a homogenous soil layer (Figure 4.33). The level of fluid in the landfill is constant at the same height as the water table in the surrounding soil. Two sampling wells are positioned 28m apart on either side of the landfill. The model simulation is defined in Figure 4.35; two dimensions are simulated.

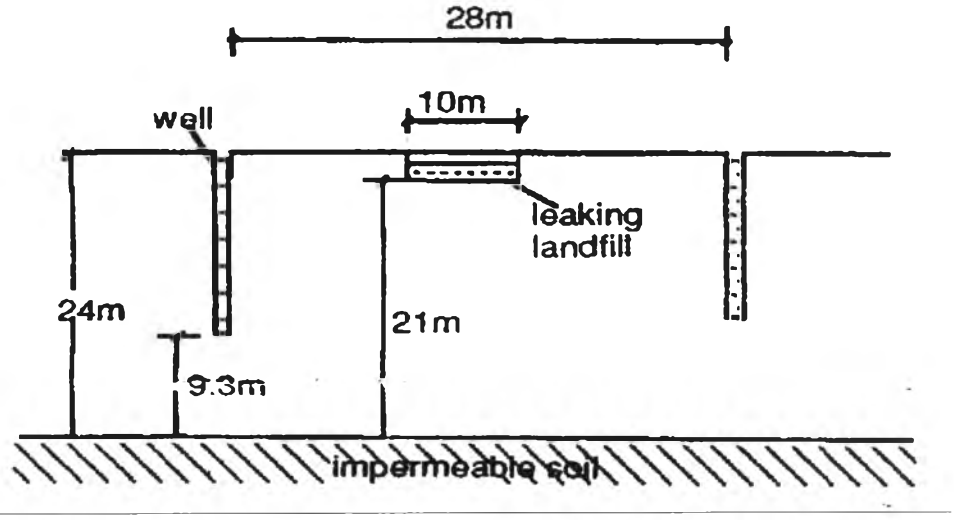

Figure 4.33 The prototype of centrifuge test (From Hellawel and Savvidou, 1994)

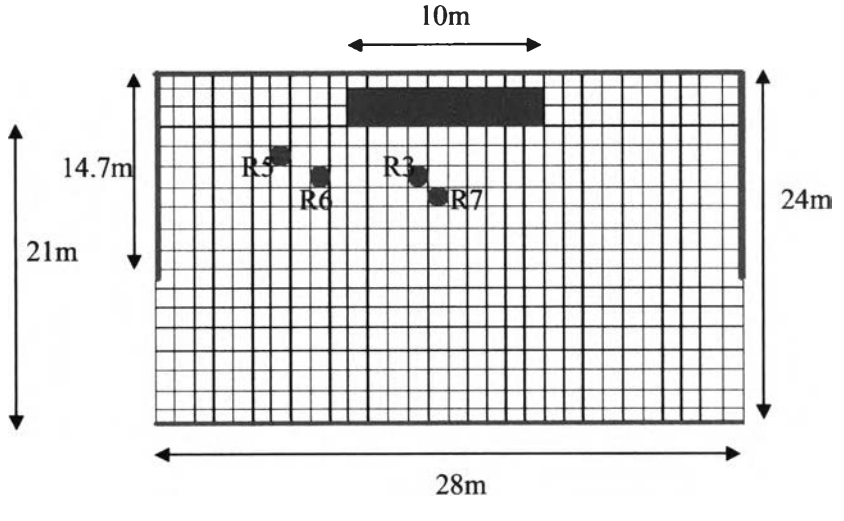

Figure 4.34 Solution domain for contaminant movement in centrifuge model test

The boundary condition for this test is set as follows;

Constant Head

Left side: start and stop time head = 24m

Right side: start and stop time head = 24m

Top side: start and stop time head = 24m

Low side: start and stop time head = 24m

Observation concentration well

R3 set at (13.42m, 7.43m)

R5 set at (7.09m, 6.64m)

R6 set at (8.68m, 7.43m)

R7 set at (14.21m, 8.36m)

At time t equal to 0 year, the model is full with Silica Flour. Then the contaminant release from the landfill and the observation concentration well are added at the different coordinates to monitor the concentration of the contaminant.

After input all the parameters into the MODFLOW program, the next step is to run the model. The method that uses in this study is Upstream Finite Difference. The result of the concentration compare with the experimental result are shown in Figure 4.35, 4.36, 4.37, 4.38, 4.39, 4.40, 4.41 and 4.42.

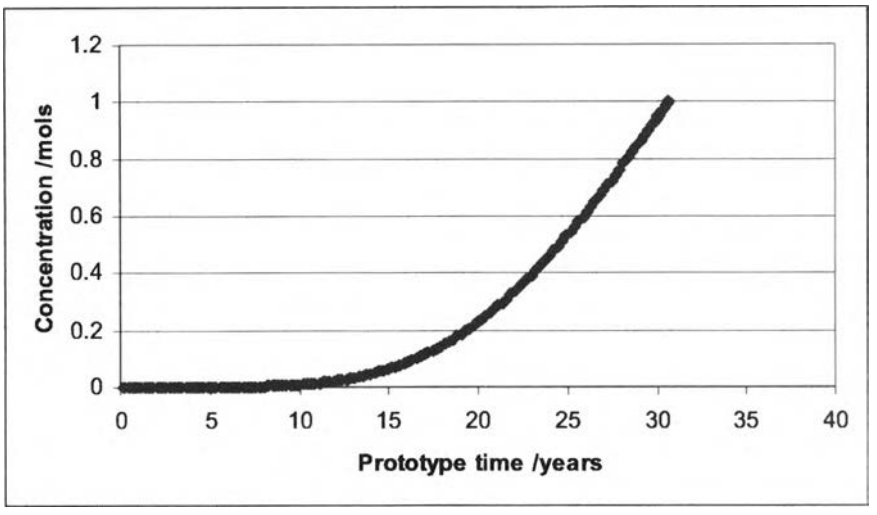

Figure 4.35 The predicted result for the movement of the contaminant at R3

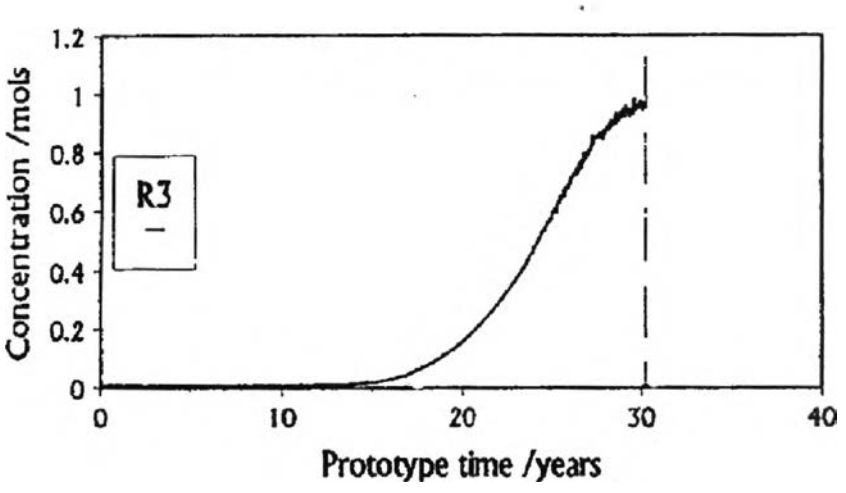

Figure 4.36 The experimental result for the movement of the concentration at R3 (From Hellawel and Savvidou, 1994)

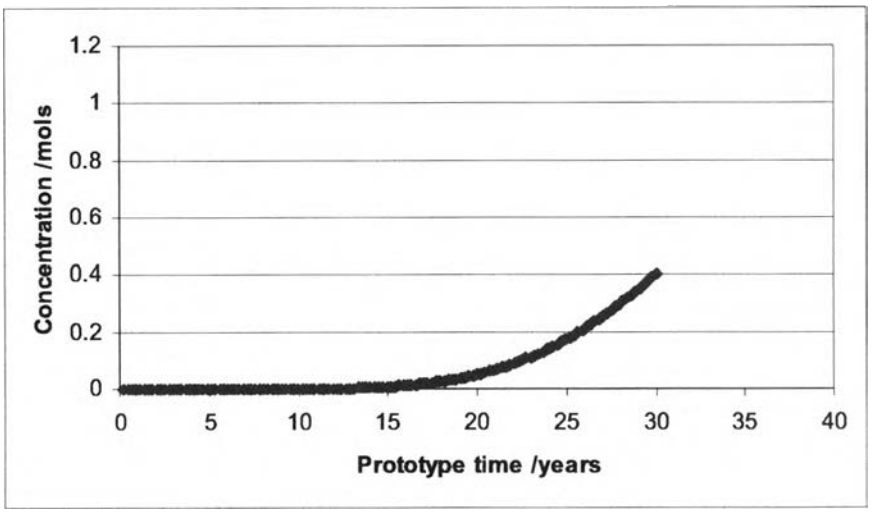

Figure 4.37 The predicted result for the movement of the contaminant at R5

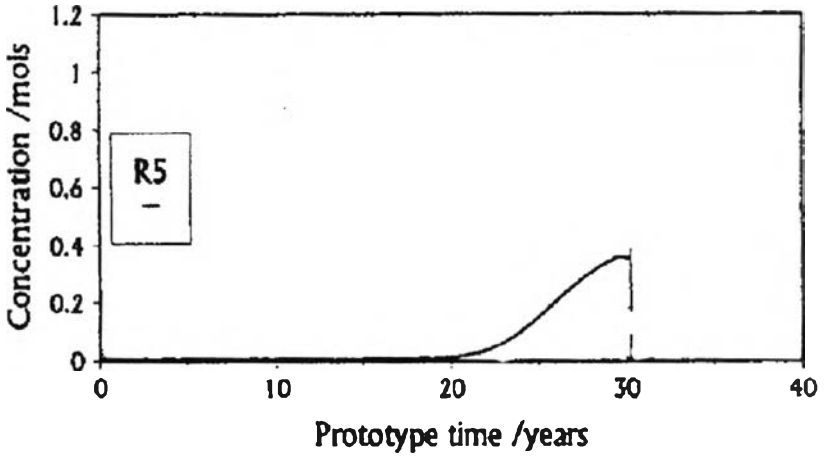

Figure 4.38 The experimental result for the movement of the concentration at R5 (From Hellawel and Savvidou, 1994)

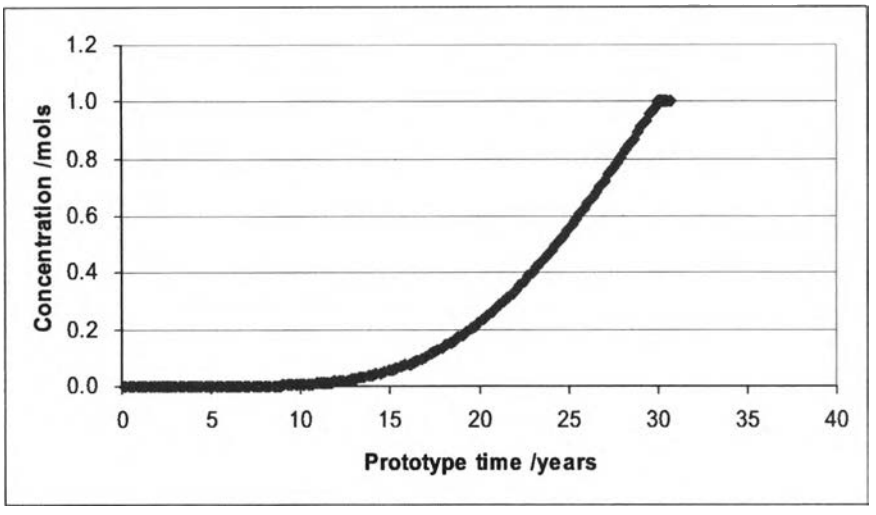

Figure 4.39 The predicted result for the movement of the contaminant at R6

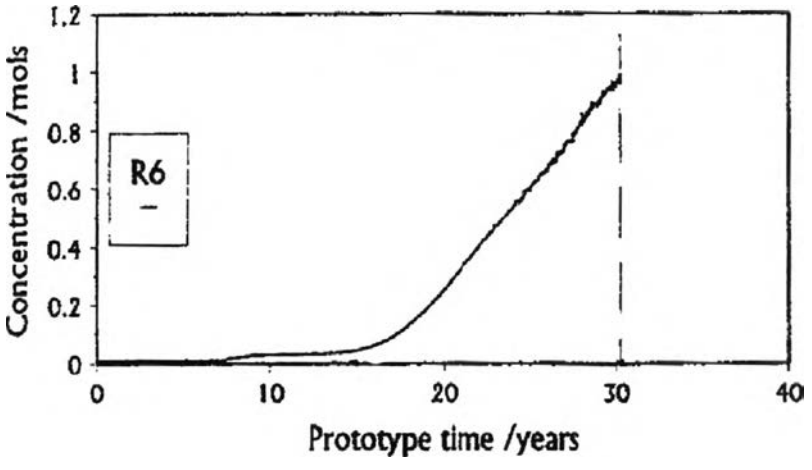

Figure 4.40 The experimental result for the movement of the concentration at R6
(From Hellawel and Savvidou, 1994)

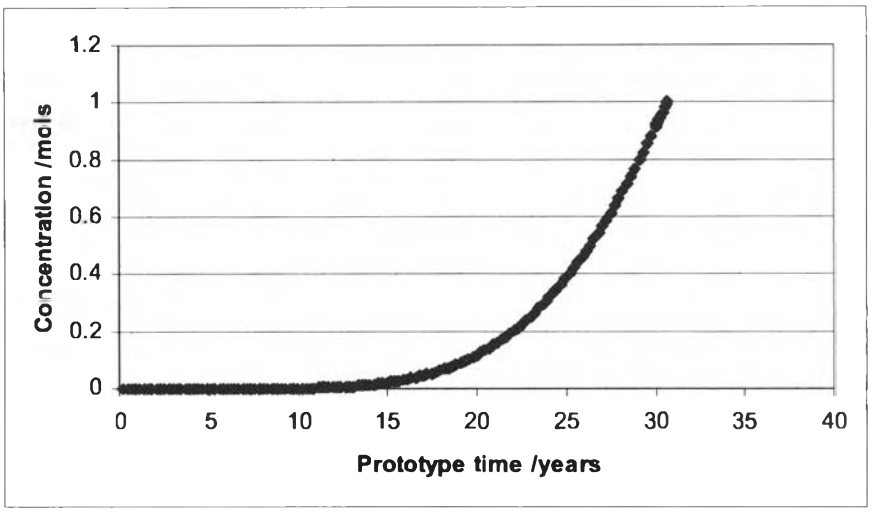

Figure 4.41 The predicted result for the movement of the contaminant at R7

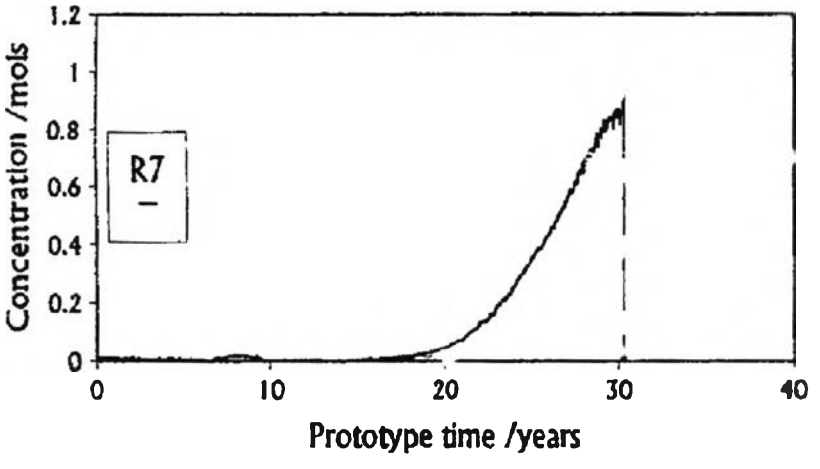

Figure 4.42 The experimental result for the movement of the concentration at R7 (From Hellawel and Savvidou, 1994)

From the Figure above, the simulation results compare reasonably well with experimental results. It shows that the program MODFLOW can be used to simulate the centrifuge model test result.